



# Warm inflation in hybrid metric-Palatini gravity under standard and irreversible thermodynamical approach

Iqra Shahid<sup>1,a</sup>, Rabia Saleem<sup>1,b</sup>, Hafiza Rizwana Kausar<sup>2,c</sup>

<sup>1</sup> Department of Mathematics, COMSATS University Islamabad, Lahore Campus, Lahore, Pakistan

<sup>2</sup> Department of Mathematics, Faculty of Science and Technology, University of Central Punjab, Lahore, Pakistan

Received: 18 July 2022 / Accepted: 4 January 2023 / Published online: 28 January 2023  
© The Author(s) 2023

**Abstract** The idea of hybrid metric-Palatini  $f(\mathcal{X})$  gravity (HMPG) is a blend of Einstein Hilbert (EH) action having non-linear function  $f(R)$  and linear scalar curvature  $R$  by Palatini gravity. The goal of this paper is to investigate the warm inflationary model (WIM) via standard and irreversible thermodynamical approach in  $f(\mathcal{X})$  gravity. We start our work by obtaining the field equations (FEs) for HMPG and then investigate the cosmic inflation in  $f(\mathcal{X})$  theory of gravity by looking at cosmic parameters such as slow-roll parameters, spectral index ( $n_s$ ), running of spectral index ( $\alpha_s$ ) and tensor-to-scalar ratio ( $r$ ). Next, the early universe is considered as an open system. The thermodynamics and dynamical equations in  $f(\mathcal{X})$  gravity are applied to interacting cosmic fluid, which leads us to adapt the basic formalism of WIM. This analysis is done using Higgs Potential (HP). Numerical results of the thermodynamical equations such as scale factor ( $a(t)$ ), scalar-field energy density ( $\rho_\phi$ ) and radiation energy density ( $\rho_\gamma$ ), number of scalar-field particles ( $n_\phi$ ) and temperature ( $T$ ) are derived and presented graphically using slow-roll approach and defining several dimensionless variables. From obtained results, we calculate cosmic parameters. In the end, we constraint the model parameters, and compare our calculated results to the Planck-2018 data.

## 1 Introduction

In the context of Riemannian geometry, the  $f(R)$  theory of gravity is the simplest modification of General Relativity (GR) such that, an EH action with an arbitrary function of the scalar curvature, replaces the Ricci scalar  $R$  [1–3]. This extended version provides a satisfactory and effective expla-

nation to the recent cosmological observations otherwise, it cannot be explained in the framework of GR, and mainly this theory come up with a feasible alternative to the cosmological constant  $\Lambda$ . The cosmological constant, which Einstein introduced in 1917, provides interpretation for the expansion of the universe. Many other modifications of GR can also define the cosmic acceleration in different manners unlike the simple approach of adding the cosmological constant into the FEs as well as to the action. The cosmic observation may also be described by modifying the EH action, in which  $f(R)$  theory gives a frame that permits Einstein gravity to be generalized easily. A scalar-field, that is non-minimally coupled to curvature can be established after applying a Legendre transformation. This framework provides a simple analysis of the theory, which allows a great use of physical as well as mathematical methods established in scalar–tensor gravity.

There are two proposed formalisms (standard metric formalism and Palatini formalism) to derive FEs in accordance with the action of  $f(R)$  gravity. In standard metric formalism, higher derivatives are obtained through FEs by varying the action with respect to the metric tensor  $g_{\mu\nu}$ , here the christoffel symbols  $\Gamma^\alpha_{\beta\gamma}$ , based on  $g_{\mu\nu}$ . While in Palatini formalism [4],  $\Gamma^\alpha_{\beta\gamma}$  and  $g_{\mu\nu}$  are considered as independent variables and the FEs are of second-order. Both approaches gave distinct FEs for a non-linear Lagrangian density in  $R$ , on the other hand, they are same under GR action. The scalar-field is not dynamical in the Palatini  $f(R)$  theory, implying that the Palatini approach does not add new degrees of freedom [5]. This fact has major implications for the theory, since it leads to the existence of infinite tidal forces on the surface of large astrophysical objects [5]. To overcome some of the drawbacks of metric and Palatini  $f(R)$  theories of gravity, the so-called  $f(\mathcal{X})$  gravity was presented in [6] and have since been extensively researched and refined. One of the key benefits of the HMPG is that it contains long-range forces in its scalar–tensor representation, which easily pass the solar

<sup>a</sup> e-mail: [ikra.2016@gmail.com](mailto:ikra.2016@gmail.com)

<sup>b</sup> e-mail: [rabiasaleem@cuilahore.edu.pk](mailto:rabiasaleem@cuilahore.edu.pk) (corresponding author)

<sup>c</sup> e-mail: [rizwana.kausar@ucp.edu.pk](mailto:rizwana.kausar@ucp.edu.pk)

system tests, and therefore there is no conflict between the theory and local measurements.

Cosmic acceleration occurs either from an undefined quantity known as dark energy (DE) with negative pressure or by modification of gravity that only emerges at cosmic scales. Additional terms in the EH action that are non-linear functions of Ricci scalar  $R$ , have always been a source to produce acceleration in the cosmic expansion [7–11]. In [12], authors determined the conditions for the cosmological viability of DE models whose Lagrangian densities  $f$  are represented in terms of the Ricci scalar  $R$ .  $f(R)$  theory is much efficient to elaborate the difference between these two formalisms. As in standard metric approach, the term  $df/dR$  acts as a dynamical self-interacting scalar-field, which satisfies a second-order differential equation in  $f(R)$ . For long-range interactions, scalar-field ( $\varphi$ ) demands very low mass in order to effect large astrophysical and cosmological scales. It is widely known that scalars have their effects on short scales because their presence is highly restrictive by solar system tests and laboratory observations until some type of screening procedure is being conducted [13–16]. A scalar–tensor description is also feasible in the Palatini case, but only when the known scalar-field satisfy an algebraic equation (not a differential equation). Later, the scalar-field appears as an algebraic function of the trace of stress-energy tensor  $T_{\mu\nu}$  as  $\varphi = \varphi(T)$ , that can speed up the late-time expansion in cosmic models [17, 18].

In literature, many WIM are discussed, which describe the distinct phases of cosmic inflation. Generally, the inflationary period has two phases: first is “slow-roll” and the second is “reheating”. It is generally assumed that at the end of inflation, the reheating process is started after the particle creation, caused by the scalar-field. Although, the WIM proposes the production of radiation without any reheating process. The cosmic inflation has also been explained in the last two decades within higher derivative curvature theories [10, 19–21], and with reference to natural inflation [22, 23], k-inflation [24], brane inflation [25] etc. The point to consider here is that, any inflationary model can be described by two well-known parameters  $r$  and  $n_s$ . Under slow-roll approximation, these parameters are written in terms of some slow-roll parameters, which can further be explained through Hubble parameter  $H$ , scalar-field  $\varphi$  and its associated potential  $V(\varphi)$ .

Zimdahl et al. [26] studied the particle production in a simple kinetic model in the expanding universe. They found that radiation and non-relativistic matter can be stable at same temperature, and the matter particles creation are at a rate of half of the expansion. Resultantly, the adiabatic creation of massive particles with an equal distribution suggested power-law inflation. However the open and irreversible processes of particle creation have not been studied sufficiently. Matter creation and annihilation processes fall into a specific kind of

open thermodynamical systems. To integrate the irreversible particle production, the standard adiabatic conservation rules needs to modified. In [27], open thermodynamical system is used for the very first time in cosmology. The classical description of this method is described in [27], investigated and further extended in [28, 29]. They [30] discussed two widely studied extensions of  $f(R)$  gravity, first is HMPG and second is modified gravity using curvature-matter couplings. Bohmer et al. [31] examined the stability of Einstein static universe by taking linear perturbations in scalar–tensor form of HMPG. In [32], authors discussed the possibility that HMPG theory can explain wormholes. They presented general conditions for wormhole solutions in context of throat’s null energy condition and provide some examples. Harko et al. [33] considered cylindrically and static symmetric interior string type solutions in scalar–tensor description of the HMPG. Tamanini and Boehmer [34] introduced a technique for modified gravity, which generalized the HMPG. In a generalised HMPG, they [35] constructed the exact solutions that describe a FLRW universe and showed that the flat universes can nevertheless have exponentially increasing solutions even if the cosmology is not fully vacuum. The mentioned approach allows specific entropy fluctuations as expected for “non-equilibrium and irreversible processes”. Recently, Saleem and Shahid [36], studied the WIM via “irreversible thermodynamics of open systems” (ITOS) under creation(decay) of matter in Rastall gravity. From this interesting idea [37], we are motivated to discuss WIM within  $f(\mathcal{X})$  gravity.

The cosmological implications of HMPG are investigated in [38, 39]. The goal of this paper is to investigate cosmic characteristics of cosmic inflation using hybrid  $f(\mathcal{X})$  theory. The governing FEs of HMPG using FRW cosmology are written in Sect. 2. In the same section, we reconstruct the above cosmic parameters in  $f(\mathcal{X})$  gravity. To obtain the graphical results, we apply perturbations to the cosmic parameters in Sect. 3. We discuss the WIM via ITOS within  $f(\mathcal{X})$  gravity using HP in Sect. 4. In Sect. 5, we conclude our results.

## 2 An overview of $f(\mathcal{X})$ gravity

The action for HMPG is given below

$$S = \int \sqrt{-g}(f(\mathbb{R}) + R + 2\kappa^2 \mathcal{L}_m) d^4x, \quad (1)$$

where  $\mathcal{L}_m$  be the matter Lagrangian,  $\kappa$  is the coupling constant whose value is  $\kappa^2 = \frac{8\pi}{M_p^2} = 1$  and  $R$  is the Einstein scalar curvature. In addition to standard form of EH action, there is an extra function  $f(\mathbb{R})$ , and the Palatini curvature  $\mathbb{R}$  concerning an independent connection  $\bar{\Gamma}$ , defined as under

$$\mathbb{R} = g^{\mu\nu} \mathbb{R}_{\mu\nu} = g^{\mu\nu} (\bar{\Gamma}_{\mu\nu,\sigma}^\sigma - \bar{\Gamma}_{\mu\sigma,\nu}^\sigma + \bar{\Gamma}_{\sigma\lambda}^\sigma \bar{\Gamma}_{\mu\nu}^\lambda - \bar{\Gamma}_{\mu\lambda}^\sigma \bar{\Gamma}_{\sigma\nu}^\lambda). \tag{2}$$

For the usual scalar curvature  $R$ , the formula will be without bar. By varying the above action as for metric tensor  $g^{\mu\nu}$ , we get the following FEs

$$G_{\mu\nu} + f_{\mathbb{R}} \mathbb{R}_{\mu\nu} - \frac{1}{2} g_{\mu\nu} f(\mathbb{R}) = T_{\mu\nu}, \tag{3}$$

with Einstein tensor  $G_{\mu\nu}$ ,  $f_{\mathbb{R}} \equiv \frac{df(\mathbb{R})}{d\mathbb{R}}$ . Now on varying Eq. (1) with respect to independent connection, we have the following equation of motion

$$\nabla_\sigma [\sqrt{-g} f_{\mathbb{R}} g^{\mu\nu}] = 0, \tag{4}$$

here  $\nabla_\sigma$  indicates the covariant derivative. Using Eq. (4), we can develop a relation between Palatini curvature tensor and usual Ricci tensor as

$$\mathbb{R}_{\mu\nu} = R_{\mu\nu} + \frac{3}{2f_{\mathbb{R}}^2} f_{\mathbb{R},\mu} f_{\mathbb{R},\nu} - \frac{1}{f_{\mathbb{R}}} \nabla_\mu f_{\mathbb{R},\nu} - \frac{g_{\mu\nu}}{2f_{\mathbb{R}}} \square f_{\mathbb{R}}. \tag{5}$$

The contraction of the above relation yields the following relation:

$$\mathbb{R} = R + \frac{3}{2} \left( \left( \frac{f_{\mathbb{R}}}{f_{\mathbb{R}}} \right)^2 - 2 \frac{\square f_{\mathbb{R}}}{f_{\mathbb{R}}} \right). \tag{6}$$

Putting the above expression in Eq. (3), we get

$$[1 + f(\mathbb{R})]G_{\mu\nu} = T_{\mu\nu} - \square f_{\mathbb{R}} g_{\mu\nu} + \nabla_\mu f_{\mathbb{R},\nu} - \frac{3}{2} \frac{f_{\mathbb{R},\mu} f_{\mathbb{R},\nu}}{f_{\mathbb{R}}} - \frac{1}{2} f_{\mathbb{R}} \mathbb{R} - f(\mathbb{R})g_{\mu\nu} + \frac{3}{4} \frac{f_{\mathbb{R},\sigma} f_{\mathbb{R}}^\sigma g_{\mu\nu}}{f_{\mathbb{R}}}. \tag{7}$$

Trace of Eq. (3) provides Palatini curvature in the following form

$$f_{\mathbb{R}} \mathbb{R} - 2f(\mathbb{R}) = T + R \equiv \mathcal{X}. \tag{8}$$

Now, the curvature  $\mathbb{R}$ , can be algebraically expressed in term of  $\mathcal{X}$ , if analytic solutions exist for the form of  $f(\mathbb{R})$ , known as  $f(\mathcal{X})$  theory of gravity. The new variable  $\mathcal{X}$  estimates that how much theory changes from the standard equation,  $R = -T$  in GR. The corresponding equations can be rewritten as  $G_{\mu\nu} = T_{\mu\nu}^{eff}$ , where  $T_{\mu\nu}^{eff} = T_{\mu\nu}^{\mathcal{X}} + T_{\mu\nu}$ , the quantity  $T_{\mu\nu}^{\mathcal{X}}$  can be defined as

$$T_{\mu\nu}^{\mathcal{X}} = \nabla_\mu \mathcal{X}_{,\nu} F'(\mathcal{X}) - R_{\mu\nu} F(\mathcal{X}) + \frac{g_{\mu\nu}}{2} \left( F'(\mathcal{X}) \square \mathcal{X} + f(\mathcal{X}) + F''(\mathcal{X})(\partial \mathcal{X})^2 \right)$$

$$+ \mathcal{X}_{,\mu} \mathcal{X}_{,\nu} \left( F''(\mathcal{X}) - \frac{3}{2} \frac{F'^2(\mathcal{X})}{F(\mathcal{X})} \right). \tag{9}$$

It is worth to mention that  $F(\mathbb{R}(\mathcal{X}))$  can be written as  $F(\mathcal{X})$  and  $F'(\mathcal{X}) = \frac{\partial F(\mathbb{R}(\mathcal{X}))}{\partial \mathcal{X}}$ . Now the trace of FEs is as follows

$$\square \mathcal{X} F'(\mathcal{X}) + \frac{1}{3} \left( 2f(\mathcal{X}) - F(\mathcal{X})R + \mathcal{X} \right) + (\partial \mathcal{X})^2 \left( F''(\mathcal{X}) - \frac{1}{2} \frac{F'(\mathcal{X})^2}{F(\mathcal{X})} \right) = 0.$$

The relation between  $R$  and  $\mathbb{R}$  in terms of  $\mathcal{X}$  is given as

$$\mathbb{R}(\mathcal{X}) = \frac{3}{2} \left[ \left( \frac{F'(\mathcal{X})}{F(\mathcal{X})} \right)^2 - \frac{2\square F(\mathcal{X})}{F(\mathcal{X})} \right] + R. \tag{10}$$

The general action (1) can be convert into a scalar-tensor representation of  $f(\mathcal{X})$  gravity by taking an arbitrary field  $\varphi$ , so that

$$S = \int \sqrt{-g} (R + f(\varphi) + f_\varphi (\mathbb{R} - \varphi) + 2\mathcal{L}_m) d^4x, \tag{11}$$

where  $f_\varphi = \frac{df}{d\varphi}$ . By defining the following expressions

$$V(\varphi) = \mathcal{X} F(\mathcal{X}) - f(\mathcal{X}), \quad \varphi = F(\mathcal{X}), \tag{12}$$

the above action becomes equivalent to our original action (1).

$$S = \int \sqrt{-g} (R + \varphi \mathbb{R} - V(\varphi) + 2\mathcal{L}_m) d^4x. \tag{13}$$

On varying the action (13) with respect to  $g^{\mu\nu}$ , the scalar-field and the connection have the following FEs:

$$R_{\mu\nu} - \frac{1}{2} (R - V(\varphi) + \varphi \mathbb{R}) g_{\mu\nu} + \varphi \mathbb{R}_{\mu\nu} = 2T_{\mu\nu}, \tag{14}$$

$$\mathbb{R} - V_\varphi = 0, \tag{15}$$

$$\nabla_\sigma [\varphi g^{\mu\nu} \sqrt{-g}] = 0. \tag{16}$$

The relation between two defined curvatures is modified as

$$\mathbb{R}_{\mu\nu} = R_{\mu\nu} - \frac{1}{\varphi} \left( \nabla_\mu \nabla_\nu \varphi + \frac{1}{2} \square \varphi g_{\mu\nu} \right) + \frac{3}{2\varphi^2} \partial_\mu \varphi \partial_\nu \varphi. \tag{17}$$

Substituting Eqs. (14) and (17) into Eq. (14), we get following equations

$$(1 + \varphi)G_{\mu\nu} = T_{\mu\nu} + \nabla_\mu \varphi_{,\nu} - \frac{3}{2} \frac{\varphi_{,\mu} \varphi_{,\nu}}{\varphi} - \square \varphi g_{\mu\nu} - \frac{1}{2} V(\varphi) g_{\mu\nu} + \frac{3}{4} \frac{\varphi_{,\sigma} \varphi^{,\sigma}}{\varphi} g_{\mu\nu}. \tag{18}$$

To investigate the WIM, we will use the above field equation in further sections.

### 3 FRW field equations and general formalism of warm inflation in HMPG

The FRW line-element for a homogeneous, isotropic and flat universe can be written as

$$ds^2 = dt^2 - a^2(t)(dx^2 + dy^2 + dz^2), \tag{19}$$

here  $a(t)$  denotes cosmic scale-factor. For perfect fluid, the energy–momentum tensor is defined as

$$T_{\mu\nu} = (\rho + p)u_\mu u_\nu - pg_{\mu\nu}, \tag{20}$$

where  $\rho = \rho_\phi + \rho_\gamma$ ,  $p = p_\phi + p_\gamma$ ,  $u_\nu$  represent total energy density, total pressure and four-velocity of the fluid, respectively. For radiation, we use the relation  $p_\gamma = \frac{\rho_\gamma}{3}$ . The hybrid FEs for the metric defined in Eq. (19) have the following form under slow-roll approximation (we can ignore radiation density by the inequality,  $\rho_\phi > \rho_\gamma$ )

$$\rho \approx \rho_\phi = 3H^2(1 + \varphi) + 3H\dot{\varphi} + V(\varphi) + \frac{3}{4}\left(\frac{\dot{\varphi}^2}{\varphi}\right), \tag{21}$$

$$p = -(1 + \varphi)(3H^2 + 2\dot{H}) + \frac{3}{4}\left(\frac{\dot{\varphi}^2}{\varphi}\right) + V(\varphi) - (1 + 2H)\dot{\varphi}. \tag{22}$$

The continuity equations for scalar-field and radiation are as follows

$$\begin{aligned} \dot{\rho}_\phi + 3H(\rho_\phi + p_\phi) &= -\Gamma\rho_\phi, \\ \dot{\rho}_\gamma + 4H\rho_\gamma &= \Gamma\rho_\phi. \end{aligned} \tag{23}$$

Usually for a standard scalar field, the quantity  $\Gamma(\rho_\phi + p_\phi) = \Gamma\dot{\varphi}^2$  is the dissipation term which is introduced phenomenologically in order to describe the nearly thermal radiation bath that is the outcome of the warm-inflationary scenario. In our case, the term  $(\rho_\phi + p_\phi)$  does not provide us a useful source term due to lengthy expressions. So we choose another useful source term  $\Gamma\rho_\phi$  [40]. During the inflationary epoch, the inflaton’s energy density is the order of the potential  $\rho_\phi \sim V(\varphi)$  (as potential term dominates the kinetic term  $V(\varphi) \gg \frac{1}{2}\dot{\varphi}^2$ ) and energy density  $\rho_\phi$  dominates over the energy density of radiation  $\rho_\phi > \rho_\gamma$ . When radiation production during warm inflation is quasi-stable, then  $\dot{\rho}_\gamma \ll 4H\rho_\gamma$ . Under these conditions, we have

$$\rho_\gamma = \frac{\Gamma}{4H}\rho_\phi = \zeta T^4,$$

where  $\zeta = \frac{\pi^2}{30}g_*$ , and the minimal super-symmetric standard model gives the number of relativistic degrees of freedom,  $g_* = 228.76$  and  $\zeta \simeq 70$  [41, 42]. The term  $T$  is the temperature of the thermal bath.

Taking derivative of Eq. (21) and combining it with Eq. (21), and substituting in equation of continuity (23) yields the following result

$$\ddot{\varphi} + 3H\dot{\varphi} - \frac{\dot{\varphi}^2}{2\varphi} + \frac{\varphi}{3}R - \frac{2\varphi V'(\varphi)}{3} = -\Gamma V(\varphi). \tag{24}$$

The Ricci scalar for the FRW metric is  $R = 12H^2 + 6\dot{H}$ .

To get this result coherent with HMPG, we are combining the FEs and matter conservation equation to obtain the relationship between effective potential  $V$  and  $R$  [43]

$$2V(\varphi) - \varphi V'(\varphi) = \frac{1}{2}(R + T) = \frac{1}{2}\mathcal{X}. \tag{25}$$

We can obtain  $R$  by taking the value of  $T$  from FEs as under

$$R = 3V(\varphi) - 2\varphi V'(\varphi) - 2\varphi V''(\varphi) + 3H\dot{\varphi} + \frac{3\dot{\varphi}^2}{4\varphi}. \tag{26}$$

Using above expression of  $R$  in Eq. (24), we obtain following relation

$$\begin{aligned} \ddot{\varphi} + 3H\dot{\varphi} - \frac{1}{2}\left(\frac{\dot{\varphi}^2}{\varphi}\right) + \varphi V(\varphi) \\ + \frac{1}{4}\dot{\varphi}^2 - \frac{2}{3}V'(\varphi)\varphi^2 + H\varphi\dot{\varphi} - \frac{2}{3}\varphi V'(\varphi) = -\Gamma V(\varphi). \end{aligned} \tag{27}$$

To solve the equation analytically, several fundamental limits such as the slow-roll limit,  $\varphi \ll 1$ ,  $\dot{\varphi}^2 \ll V(\varphi)$  and  $\ddot{\varphi} \ll 3H\dot{\varphi}$  can be applied on Eq. (27). The evolution of  $\varphi$  is expressed as

$$\dot{\varphi} = -\frac{\Gamma V(\varphi)}{(1 + \varphi)} + \frac{\varphi}{3H(1 + \varphi)}\left(2V'(\varphi) - V(\varphi)\right). \tag{28}$$

Utilizing above expression, Eq. (21) is turn out to be

$$3H^2 = \frac{1}{(1 + \varphi)^2}\left(2\varphi V'(\varphi) - \Gamma V(\varphi)\left(1 + \frac{\varphi}{\Gamma}\right)\right). \tag{29}$$

Similarly, Eq. (21) yields

$$\begin{aligned} \dot{H} = \frac{V(\varphi)}{1 + \varphi} - \frac{1}{2(1 + \varphi)^2}\left(2\varphi V'(\varphi) - \Gamma V(\varphi)\left(1 + \frac{\varphi}{\Gamma}\right)\right) \\ + \frac{1}{4}\left(2V'(\varphi) - V(\varphi)\left(1 + \frac{\Gamma}{\varphi}\right)\right). \end{aligned} \tag{30}$$

Inflation can be explained via quasi de-Sitter results, where the Hubble parameter  $H$  is relatively constant.

Amount of inflation is counted by number of e-foldings, defined as

$$N = \int_t^{t_e} H dt = \int_{\phi}^{\phi_e} \frac{H}{\dot{\phi}} d\phi = \ln(1 + \phi_e) - \ln(1 + \phi), \tag{31}$$

where  $\phi_e$  denotes the value of inflaton at the end of inflation. The slow-roll parameters can be defined as follows to observe the inflation under slow-roll limit [44–46]

$$\epsilon_1 = -\frac{\dot{H}}{H^2}, \quad \eta = \frac{\ddot{\phi}}{H\dot{\phi}}. \tag{32}$$

In  $f(\mathcal{R})$  theory of gravity,  $\epsilon_1$  and  $\eta$  take the following form

$$\epsilon_1 = \frac{3}{2} - \frac{3(1 + \phi) \left( V(\phi) + \frac{1}{4} \left( 2V'(\phi) - V(\phi) \left( 1 + \frac{\Gamma}{\phi} \right) \right) \right)}{\left( 2\phi V'(\phi) - \Gamma V(\phi) \left( 1 + \frac{\phi}{\Gamma} \right) \right)}, \tag{33}$$

$$\begin{aligned} \eta = (1 + \phi) & \left( \frac{V'(\phi)}{1 + \phi} - \frac{V(\phi)}{(1 + \phi)^2} - \frac{1}{2(1 + \phi)^2} \left( 2V'(\phi) \right. \right. \\ & + 2\phi V''(\phi) - \left. \left. \left( \Gamma' V(\phi) + \Gamma V'(\phi) \right) \left( 1 + \frac{\phi}{\Gamma} \right) \right) \right. \\ & - \left. \left( 1 - \frac{\Gamma'}{\Gamma} \right) V(\phi) \right) \left( 2\phi V'(\phi) - \Gamma V(\phi) \left( 1 + \frac{\phi}{\Gamma} \right) \right) \\ & + \frac{1}{4} \left( 2V''(\phi) - \left( 1 + \frac{\Gamma}{\phi} \right) V'(\phi) - \frac{V(\phi)}{\phi} \left( \Gamma' - \frac{\Gamma}{\phi} \right) \right) \\ & \times \left( \frac{V(\phi)}{1 + \phi} - \frac{1}{2(1 + \phi)^2} \left( 2\phi V'(\phi) - \Gamma V(\phi) \left( 1 + \frac{\phi}{\Gamma} \right) \right) \right) \\ & + \frac{1}{4} \left( 2V'(\phi) - \left( 1 + \frac{\Gamma}{\phi} \right) V(\phi) \right)^{-1}. \end{aligned} \tag{34}$$

It is important to mention that the slow-roll parameters must have minimum values to display inflation. In the consequence of this fact, we require  $\dot{H} < 0$  by which  $0 < \epsilon_1 \ll 1$ , and also  $0 < \eta \ll 1$ . When  $\epsilon_1 \simeq 1$ , it is the time when inflation era ends.

At the end of inflation where  $\epsilon_1 = 1$ , we get a first order non-linear differential equation in  $V(\phi)$  from Eq. (33), whose solution is calculated as

$$T = \frac{\Gamma \left( 3e^{\frac{4\Gamma\phi + \Gamma - 26\phi^3}{4\phi^2}} \left( \frac{\phi + 3}{\phi} \right)^{-\frac{2\Gamma}{9}} \right)}{(4\zeta)A(\phi)}, \tag{38}$$

$$P_s = -\frac{A(\phi) \left( \Gamma (3\phi^3 + 11\phi^2 + 21\phi + 9) + 6(7\phi + 9)\phi^3 \right)^2 \sqrt{\frac{\pi\Gamma}{A(\phi)} + \pi} \left( \frac{\Gamma e^{\frac{4\Gamma\phi + \Gamma - 26\phi^3}{4\phi^2}} \left( \frac{\phi + 3}{\phi} \right)^{-\frac{2\Gamma}{9}}}{\zeta A(\phi)} \right)^{\frac{1}{4}}}{2^{3/2} 3^{3/4} (\phi + 1)^2 \left( -3\Gamma(\phi + 3)\phi^2 A(\phi) + \Gamma(2\phi^2 + 21\phi + 9) + 6(7\phi + 9)\phi^3 \right)^2}, \tag{39}$$

$$r = \frac{(\phi + 1)^2 A(\phi) \left( 72\phi^2(\phi + 3)^2 A(\phi) + \sqrt{6} (54\phi^4 + 37\phi^3 - 108\phi^2 - 288\phi - 108) \right)^2}{48 \cdot 2^{3/8} 3^{7/8} \pi^{5/2} (\phi + 3)^2 (11\phi^2 + 21\phi + 9)^2 \sqrt{1 - \frac{2\sqrt{6}}{A(\phi)} \left( \frac{(\phi + 3)(\phi^2 + \phi)^2 A(\phi)}{g(7\phi^4 + 3\phi^3 - 22\phi^2 - 42\phi - 18)} \right)^{\frac{1}{4}}}}. \tag{40}$$

$$\begin{aligned} V(\phi) &= \exp \left[ - \int \left( \frac{12(1 + \phi) + \Gamma \left( 5 + \left( \frac{\phi + 3}{\Gamma} \right) + \frac{3}{\phi} \right) \right)}{2(\phi + 3)} d\phi \right], \\ &= \exp \left[ \ln(\phi + 3)^{12} - \frac{13}{2}\phi - \frac{\Gamma_0 T^3}{2} \right. \\ &\quad \left. \times \left( \ln \left( \frac{\phi + 3}{\phi} \right)^{\frac{4}{9}} - \frac{1}{2\phi^2} (1 + 4\phi) \right) \right]. \end{aligned} \tag{35}$$

The dissipation factor is chosen to be  $\Gamma = \Gamma_0 T^3$ . The inflaton can be written in terms of e-foldings using following relation

$$\phi = (\phi_e + 1) \exp[N] - 1. \tag{36}$$

Perturbation spectra analysis in WIM have been thoroughly studied in [41,47,48] for both constant and temperature-dependent. The following independent parameters are utilized to examine the power spectrum of primordial fluctuations in inflationary scenario, and to compare the underlined model with standard data. These parameters are denoted by  $P_s$  (scalar power spectrum),  $P_t$  (tensor power spectrum),  $r$ ,  $n_s$  and  $\alpha_s$ . The definition of these parameters are given below:

$$\begin{aligned} P_s &= \frac{\sqrt{\pi}}{2} \left( \frac{H^3 T}{\dot{\phi}^2} \left( 1 + \frac{\Gamma}{3H} \right)^2 \right), \quad P_t = \frac{H^2}{2\pi^2 M_{Pl}^2}, \\ r &= \frac{P_t}{P_s}, \quad n_s = 1 + \frac{d \ln P_s}{d \ln k}, \quad \alpha_s = \frac{dn_s}{d \ln k}, \end{aligned} \tag{37}$$

where  $k$  is the wave number, which is related to e-folding number  $N$  via  $dN = d \ln k$ . For HMPG,  $T$ ,  $P_s$  and  $r$  is evaluated as

The scalar spectral index for  $f(\mathcal{X})$  gravity is obtained as

$$\begin{aligned}
 n_s = & 1 - \left( -24e^{\frac{4\varphi\Gamma+\Gamma}{4\varphi^2}} (\varphi + 1) \left( 13\varphi^3 + 2\Gamma\varphi + \Gamma \right) \right. \\
 & \times \left( 6(7\varphi + 9)\varphi^3 + \Gamma \left( 3\varphi^3 + 11\varphi^2 + 21\varphi + 9 \right) \right) (\Gamma + A(\varphi)) \\
 & \times \left( 6\varphi^3(7\varphi + 9) - \Gamma \left( 3A(\varphi)\varphi^3 + (9A(\varphi) - 2)\varphi^2 - 21\varphi - 9 \right) \right) \\
 & + 576e^{\frac{4\varphi\Gamma+\Gamma}{4\varphi^2}} \varphi^3(\varphi + 1) \left( 6(7\varphi + 9)\varphi^3 \right. \\
 & + \Gamma \left( 3\varphi^3 + 11\varphi^2 + 21\varphi + 9 \right) \left. \right) (\Gamma + A(\varphi)) \left( 6\varphi^3(7\varphi + 9) \right. \\
 & - \Gamma \left( 3A(\varphi)\varphi^3 + (9A(\varphi) - 2)\varphi^2 - 21\varphi - 9 \right) \left. \right) \\
 & + 3e^{\frac{4\varphi\Gamma+\Gamma}{4\varphi^2}} \left( 18 \left( 91\varphi^4 + 299\varphi^3 + 335\varphi^2 + 165\varphi + 54 \right) \right. \\
 & \varphi^5 + 3\Gamma \left( 900\varphi^4 + 1400\varphi^3 + 681\varphi^2 - 99\varphi - 108 \right) \varphi^2 \\
 & + \Gamma^2 \left( 385\varphi^4 + 858\varphi^3 + 936\varphi^2 + 459\varphi + 81 \right) \left. \right) \\
 & (\Gamma + A(\varphi)) \left( 6\varphi^3(7\varphi + 9) \right. \\
 & - \Gamma \left( 3A(\varphi)\varphi^3 + (9A(\varphi) - 2)\varphi^2 - 21\varphi - 9 \right) \\
 & + \left. \left( 6\varphi^3(7\varphi + 9) - \Gamma \left( 3A(\varphi)\varphi^3 + (9A(\varphi) - 2)\varphi^2 - 21\varphi - 9 \right) \right) \right) \\
 & \left/ \left( 16 \left( 6(7\varphi + 9)\varphi^3 + \Gamma(3\varphi^3 + 11\varphi^2 + 21\varphi + 9) \right) \right)^2 \right. \\
 & \left. \left( \frac{\Gamma}{A(\varphi)} + 1 \right) \left( 6\varphi^3(7\varphi + 9) \right. \right. \\
 & \left. \left. - \Gamma \left( 3A(\varphi)\varphi^3 + (9A(\varphi) - 2)\varphi^2 - 21\varphi - 9 \right) \right)^3 \right), \tag{41}
 \end{aligned}$$

where

$$A(\varphi) = \left( \frac{e^{\frac{4\Gamma\varphi+\Gamma-26\varphi^3}{4\varphi^2}} \left( \frac{\varphi+3}{\varphi} \right)^{-\frac{2\Gamma}{9}} \left( \Gamma(3\varphi^3 + 11\varphi^2 + 21\varphi + 9) + 6(7\varphi + 9)\varphi^3 \right)}{\varphi^2(\varphi + 1)^2} \right)^{\frac{1}{2}} \tag{42}$$

Putting expressions of  $V(\varphi)$  and  $\varphi$ , we can develop the aforementioned inflationary observables ( $r, n_s, \alpha_s$ ) in terms of e-foldings. The parametric plots of  $r - n_s$  and  $\alpha_s - n_s$  are shown in Fig. 1. It can be seen clearly from the plot that the value of  $r$  at  $n_s = 0.968$  is less than the standard observed value of  $r$ , i.e.,  $r < 0.056$ . The results are well-consistent with Planck-2018 data. The running of the spectral-index  $\alpha_s$  in WIM is of second-order in inflationary slow-roll parameters and is often minimal  $\alpha_s \approx 10^{-3}$ . Therefore, by simultaneous attaining a sufficient number of e-folds, it may be feasible to design some models capable of producing a large running over a wave number  $k$  attainable to CMB observations [49].

#### 4 Higgs potential with irreversible scalar-field and radiation interaction

In the process of particle creation, the number of particles and the energy momentum of a fluid’s components are not independently conserved. In these type of fluids, momentum and energy can be exchanged within components of fluids. We assume that number densities of a particle  $n_\varphi$  and  $n_\gamma$  fulfill the balance laws, which is given below:

$$\dot{n}_\varphi + 3Hn_\varphi = -\Gamma \frac{\rho_\varphi}{m_\varphi}, \tag{43}$$

$$\dot{n}_\gamma + 3Hn_\gamma = \Gamma \frac{\rho_\varphi}{m_\varphi}, \tag{44}$$

where  $m_\varphi$  denotes scalar-field particle mass.

In analytical formalism of irreversible thermodynamical process with particle creation or decay, the thermodynamic pressure appears naturally because of the variation in particle numbers, i.e., creation pressure. The general expression for the creation pressure  $p_c$ , is

$$p_c = -\frac{h}{3nH}(\dot{n} + 3nH), \tag{45}$$

where  $h = \rho + p$ . The total heat ( $h$ ) of radiation and scalar-field are given by  $h_\gamma = \rho_\gamma + p_\gamma$  and  $h_\varphi = \rho_\varphi + p_\varphi$ , respectively. By using the conservation Eqs. (43) and (44) in above equation, we have the following relations

$$\begin{aligned}
 p_c^\varphi &= \frac{\Gamma(\rho_\varphi + p_\varphi)\rho_\varphi}{3Hm_\varphi n_\varphi}, \\
 p_c^\gamma &= -\frac{\Gamma(\rho_\gamma + p_\gamma)\rho_\varphi}{3Hm_\varphi n_\gamma},
 \end{aligned}$$

where  $n_\gamma = 16\pi\zeta(3)\mathcal{T}^3$ ,  $\mathcal{T}$  is temperature and  $\zeta(3)$  is the “Riemann zeta function”. From Gibbs equation used in [37], we have the following conservation equation as

$$\dot{\rho}_\gamma + 3H(\rho_\gamma + p_\gamma) = \frac{\Gamma(\rho_\gamma + p_\gamma)\rho_\varphi}{m_\varphi n_\gamma}, \tag{46}$$

now putting the expression of  $p_c^\gamma$  in Eq. (46), we obtain the evolution equation of temperature  $\mathcal{T}$  as under

$$\dot{\mathcal{T}} + H\mathcal{T} = \frac{\Gamma\rho_\varphi}{48\pi\zeta(3)m_\varphi\mathcal{T}^2}. \tag{47}$$

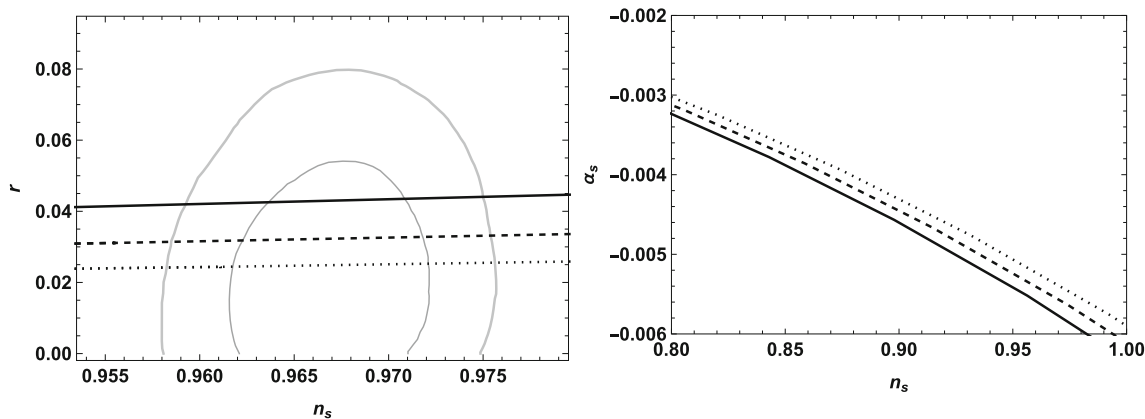


**Fig. 1** Left  $r - n_s$  parametric plot and right parametric plot is for running of spectral index  $\alpha_s - n_s$  for  $\Gamma_0 = 0.002$  (solid),  $\Gamma_0 = 0.004$  (dashed),  $\Gamma_0 = 0.006$  (dotted), which is well-fitted with Planck 2018 data [50,51]

In this section, we will use the Higgs self-interaction potential  $V(\varphi)$ , which is given below

$$V(\varphi) = \pm \frac{\nu^2}{2} \varphi^2 + \frac{\zeta}{4} \varphi^4, \tag{48}$$

where  $\nu$  and  $\zeta$  are constants.  $\zeta$  is self-coupling constant of HP and has a value  $\zeta \approx 1/8$  [52]. Now, by using the HP in cosmological evolution equations of WIM with irreversible radiation creation in  $f(\mathcal{X})$  gravity, we get following set of equations

$$3H^2 = \rho_\gamma + \frac{\dot{\varphi}^2}{2} - \frac{\varphi^2}{(1+\varphi)} \left( 2(\pm \nu^2 + \zeta \varphi^2) - (\pm \frac{\nu^2}{2} + \frac{\zeta}{4} \varphi^2)(\varphi + \Gamma) \right), \tag{49}$$

$$\dot{n}_\varphi + 3Hn_\varphi = -\frac{\Gamma}{m_\varphi} \left( \pm \frac{\nu^2}{2} \varphi^2 + \frac{\zeta}{4} \varphi^4 \right), \tag{50}$$

$$\dot{\rho}_\gamma + 4H\rho_\gamma = \Gamma \left( \pm \frac{\nu^2}{2} \varphi^2 + \frac{\zeta}{4} \varphi^4 \right), \tag{51}$$

$$\dot{T} + HT = \frac{\Gamma}{48T^2\pi\zeta(3)m_\varphi} \left( \pm \frac{\nu^2}{2} \varphi^2 + \frac{\zeta}{4} \varphi^4 \right). \tag{52}$$

To simplify the above equation, we are using the following set of dimensionless variables as

$$t = \frac{\tau}{\Gamma}, \quad \rho_\gamma = \Gamma^2 R_\gamma, \quad n_\varphi = \frac{\Gamma^2 N_\varphi}{m_\varphi}, \quad \varepsilon^2 = \frac{\nu^2}{2\Gamma^2},$$

$$\sigma = \frac{\zeta}{4\Gamma^2}$$

$$\mathcal{T} = \left( \frac{\Gamma^2}{48\pi\zeta(3)m_\varphi} \right)^{\frac{1}{3}} \vartheta, \quad u = \frac{d\vartheta}{d\tau}.$$

Using above dimensionless variables, the system of Eqs. (49)–(52) is modified to

$$\frac{da}{d\tau} = \frac{a}{\sqrt{3}} \sqrt{R_\gamma + \frac{u^2}{2} - \frac{\pm 4\varepsilon^2\varphi^2 + 8\sigma\varphi^4}{(1+\varphi)} - \frac{(\varphi + \Gamma)(\pm \varepsilon^2\varphi^2 + \sigma\varphi^4)}{(1+\varphi)}}, \tag{53}$$

$$\frac{dN_\varphi}{d\tau} + \sqrt{3} \sqrt{R_\gamma + \frac{u^2}{2} - \frac{\pm 4\varepsilon^2\varphi^2 + 8\sigma\varphi^4}{(1+\varphi)} - \frac{(\varphi + \Gamma)(\pm \varepsilon^2\varphi^2 + \sigma\varphi^4)}{(1+\varphi)}} N_\varphi = -(\pm \varepsilon\varphi^2 + \sigma\varphi^4), \tag{54}$$

$$\frac{dR_\gamma}{d\tau} + \frac{4}{\sqrt{3}} \sqrt{R_\gamma + \frac{u^2}{2} - \frac{\pm 4\varepsilon^2\varphi^2 + 8\sigma\varphi^4}{(1+\varphi)} - \frac{(\varphi + \Gamma)(\pm \varepsilon^2\varphi^2 + \sigma\varphi^4)}{(1+\varphi)}} R_\gamma = \pm \varepsilon\varphi^2 + \sigma\varphi^4, \tag{55}$$

$$\frac{d\vartheta}{d\tau} + \frac{1}{\sqrt{3}} \sqrt{R_\gamma + \frac{u^2}{2} - \frac{\pm 4\varepsilon^2\varphi^2 + 8\sigma\varphi^4}{(1+\varphi)} - \frac{(\varphi + \Gamma)(\pm \varepsilon^2\varphi^2 + \sigma\varphi^4)}{(1+\varphi)}} \vartheta = \frac{\beta}{\vartheta^2} (\pm \varepsilon^2\varphi^2 + \sigma\varphi^4). \tag{56}$$

Above Eqs. (53)–(56) can be integrated under feasible initial conditions. For numerical integration, we assume numerical values as initial conditions using HP. The values are  $a(0) = 10^{-3}$ ,  $R_\gamma(0) = 10^2$ ,  $N_\varphi(0) = 10^5$ ,  $u(0) = -1.25$ , and  $\vartheta(0) = 1.4$ .

In Fig. 2, left plot is for the case when HP is  $V(\varphi) = -\frac{\nu^2}{2}\varphi^2 + \frac{\zeta}{4}\varphi^4$  with  $\nu > 0$ , having scale factor that is a time dependent function and continuously increasing in the early stages of expansion, while for right graph when HP is of the type  $V(\varphi) = +\frac{\nu^2}{2}\varphi^2 + \frac{\zeta}{4}\varphi^4$  with  $\nu > 0$ , showing monotonically increasing behavior and appear as dependent on  $\varepsilon$ .

The dimensionless time variation and particle number of scalar-field is represented in Fig. 3. For both cases of HP with  $\nu > 0$ , it shows decreasing behavior verses time with dependence on  $\varepsilon$ .

The dimensionless time variation of radiation energy density for both cases of HP in Fig. 4. Initially, the radiation energy density is increasing due to the transfer of energy from scalar-field to the photons, and after a limited time of interval it reaches to its maximum value.

The dimensionless time variation of temperature for both cases of HP is shown in Fig. 5. In early stages, the temperature is increasing, after some short time of interval, it begins to increase rapidly.

In our next step, we will look into the scenario of HP driven inflation. Equations (49)–(52) represent the evolution equations of scalar-field  $\varphi$  and cosmological fluid. Now, we will introduce some following approximations. First, we consider that the photon fluid’s energy density is dominated by the scalar-field’s energy density. Second, we suppose scalar-field’s kinetic term is too small as opposed to its potential term, leading to,  $\rho_\varphi \gg \rho_\gamma$  and  $\rho_\varphi = G(\varphi)$ . Similarly, the constraints we have in cold inflation and throughout inflationary expansion, we suppose the photon production rate to be quasi stable, such that  $\rho_\varphi \ll H\rho_\gamma$  and  $\dot{\rho}_\gamma \ll \Gamma\dot{\varphi}$  respectively.

By using the HP, we have following expressions for  $P_s$ ,  $r$  and  $n_s$

$$P_s = \frac{3^{5/8} \sqrt{\pi} (\varphi + 1)^2 B^3(\varphi) \left( \frac{2\Gamma}{\sqrt{3}B(\varphi)} + 1 \right)^{\frac{1}{2}} \left( \frac{\Gamma\varphi^2(2\nu^2 + \zeta\varphi^2)}{\zeta B(\varphi)} \right)^{\frac{1}{4}}}{16 \cdot 2^{3/4} \left( \frac{3}{4}\Gamma(2\nu^2\varphi^2 + \zeta\varphi^4) - \frac{\sqrt{3}\varphi^2(2\nu^2(\varphi-4) + \zeta(\varphi-8)\varphi^2)}{2B(\varphi)} \right)^2}, \tag{57}$$

$$r = \frac{\varphi^6 (2\nu^2(\varphi - 3) + \zeta(\varphi - 7)\varphi^2) \left( 2\sqrt{3} (2\nu^2(\varphi - 4) + \zeta(\varphi - 8)\varphi^2) - 3\Gamma B(\varphi) (2\nu^2 + \zeta\varphi^2) \right)^2}{12 \sqrt[4]{2} \sqrt[8]{3} \pi^{5/2} (\varphi + 1)^4 B^5(\varphi) \left( \frac{2\sqrt{3}\Gamma}{B(\varphi)} + 3 \right)^{\frac{1}{2}} \left( \frac{\Gamma\varphi^2(2\nu^2 + \zeta\varphi^2)}{\zeta B(\varphi)} \right)^{\frac{1}{4}}}, \tag{58}$$

and

$$n_s = 1 - \left( 4 \left( \frac{3}{4}\Gamma(\zeta\varphi^4 + 2\nu^2\varphi^2) - \frac{\sqrt{3}\varphi^2(2(\varphi - 4)\nu^2 + \zeta(\varphi - 8)\varphi^2)}{2B(\varphi)} \right)^3 \times \left( -\sqrt{3} (3B(\varphi) + 2\Gamma\sqrt{3}) \left( 4(3\varphi^2 - 15\varphi + \Gamma(4\varphi + 2) - 8)\nu^4 + 4\zeta\varphi^2 (4\varphi^2 - 22\varphi + \Gamma(5\varphi + 3) - 12)\nu^2 + \zeta^2\varphi^4 (5\varphi^2 - 45\varphi + \Gamma(6\varphi + 4) - 32) \right) \right) \times \left( (6\Gamma B(\varphi) - 4\sqrt{3}\varphi + 16\sqrt{3})\nu^2 + \zeta\varphi^2 (3\Gamma B(\varphi) - 2\sqrt{3}\varphi + 16\sqrt{3}) \right) \varphi^3 + 16 (2\nu^2 + \zeta\varphi^2) \left( 2(\Gamma + \varphi - 4)\nu^2 + \zeta\varphi^2(\Gamma + \varphi - 8) \right) \left( 3B(\varphi) + 2\Gamma\sqrt{3} \right) \left( 2\sqrt{3}\varphi^2 (2(\varphi - 4)\nu^2 + \zeta(\varphi - 8)\varphi^2) - 3\Gamma(\zeta\varphi^4 + 2\nu^2\varphi^2) B(\varphi) \right) \sqrt{3}\varphi^2 - 16\sqrt{3} (2\nu^2 + \zeta\varphi^2) \left( 3B(\varphi) + 2\Gamma\sqrt{3} \right) \left( 2(\varphi + 1) (2(\Gamma + \varphi - 4)\nu^2 + \zeta\varphi^2(\Gamma + \varphi - 8)) (2\nu^2 + \zeta\varphi(3\varphi - 16)) \times \sqrt{3}\varphi^3 + 4(\varphi + 1) (2(\varphi - 4)\nu^2 + \zeta(\varphi - 8)\varphi^2) \right) \times \left( 2(\Gamma + \varphi - 4)\nu^2 + \zeta\varphi^2(\Gamma + \varphi - 8) \right) \sqrt{3}\varphi^2 - \sqrt{3} (2(\varphi - 4)\nu^2 + \zeta(\varphi - 8)\varphi^2) \times \left( \zeta (3\varphi^2 - 11\varphi + 2\Gamma(\varphi + 2) - 32) \varphi^3 + 2\nu^2 (\varphi^2 + 3\varphi + 2\Gamma - 8) \varphi + 12\Gamma(\varphi + 1)^3 (\nu^2 + \zeta\varphi^2) \times B^3(\varphi) \right) \varphi - 12\Gamma (2\nu^2 + \zeta\varphi^2) \left( \zeta (3\varphi^2 - 11\varphi + 2\Gamma(\varphi + 2) - 32) \varphi^3 + 2\nu^2 (\varphi^2 + 3\varphi + 2\Gamma - 8) \varphi \right) \left( 2\sqrt{3}\varphi^2 \times (2(\varphi - 4)\nu^2 + \zeta(\varphi - 8)\varphi^2) - 3\Gamma (\zeta\varphi^4 + 2\nu^2\varphi^2) B(\varphi) \right) + 12 (2\nu^2 + \zeta\varphi^2) \left( \zeta (3\varphi^2 - 11\varphi + 2\Gamma(\varphi + 2) - 32) \varphi^3 + 2\nu^2 (\varphi^2 + 3\varphi + 2\Gamma - 8) \varphi \right) \left( 3B(\varphi) + 2\Gamma\sqrt{3} \right) \times \left( 2\sqrt{3}\varphi^2 (2(\varphi - 4)\nu^2 + \zeta(\varphi - 8)\varphi^2) - 3\Gamma (\zeta\varphi^4 + 2\nu^2\varphi^2) B(\varphi) \right) \sqrt{3} \right) \left( 9\varphi^2(\varphi + 1)^2 (2\nu^2 + \zeta\varphi^2) \times (2(\Gamma + \varphi - 4)\nu^2 + \zeta\varphi^2(\Gamma + \varphi - 8)) \times \left( \frac{2\Gamma}{\sqrt{3}B(\varphi)} + 1 \right) \left( 2\sqrt{3}\varphi^2 (2(\varphi - 4)\nu^2 + \zeta(\varphi - 8)\varphi^2) - 3\Gamma (\zeta\varphi^4 + 2\nu^2\varphi^2) B(\varphi) \right)^3 \right), \tag{59}$$



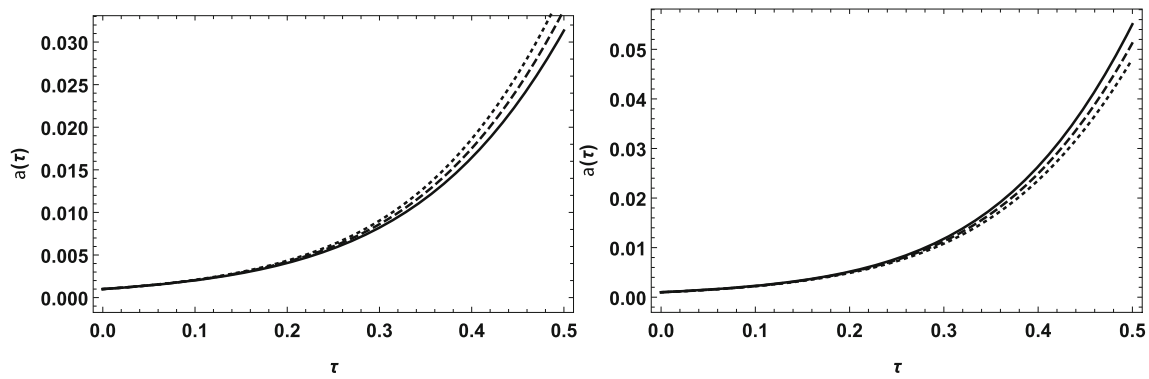


**Fig. 2** Above plots show the scale factor versus dimensionless time. Left plot is for  $V(\varphi) = -\frac{v^2}{2}\varphi^2 + \frac{\xi}{4}\varphi^4$  and right plot is for  $V(\varphi) = +\frac{v^2}{2}\varphi^2 + \frac{\xi}{4}\varphi^4$ . Here we fixed the  $\sigma = 0.76$ ,  $\Gamma = 0.2$  with the different values of  $\varepsilon$ ,  $\varepsilon = 0.8$  (solid curve),  $\varepsilon = 0.6$  (dashed curve) and  $\varepsilon = 0.4$  (dotted curve)

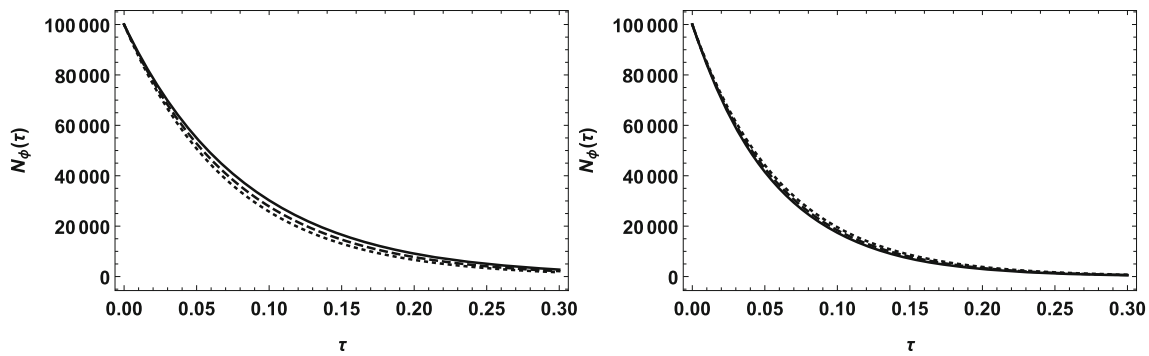


**Fig. 3** Above plots show the scalar-field particle number,  $N_\varphi$  versus dimensionless time. Left plot is for  $V(\varphi) = -\frac{v^2}{2}\varphi^2 + \frac{\xi}{4}\varphi^4$  and right plot is for  $V(\varphi) = +\frac{v^2}{2}\varphi^2 + \frac{\xi}{4}\varphi^4$ . Here we fixed the  $\sigma = 0.76$ ,  $\Gamma = 0.2$  with the different values of  $\varepsilon$ ,  $\varepsilon = 0.8$  (solid curve),  $\varepsilon = 0.6$  (dashed curve) and  $\varepsilon = 0.4$  (dotted curve)

where

$$B(\varphi) = \left( \frac{\varphi^2 (2v^2(\Gamma + \varphi - 4) + \xi\varphi^2(\Gamma + \varphi - 8))}{(\varphi + 1)^2} \right)^{\frac{1}{2}}.$$

In above figures  $r - n_s$  and  $n_s - \alpha_s$ , show that it is fitted well with Planck 2018 results (TT, TE, EE + LowE + Lensing + BK14 + BAO) [50,51].

### 5 Summary

To examine cosmological inflation, we have used HMPG model. In this theory the FEs were constructed by taking  $\mathcal{X} = R + T$ , so the matter and curvature can be studied together. These theories have been given in the literature as an alternate to DM and DE, and they have been proved to be compatible with local solar system test. Not only does inflation anticipate a flat, homogeneous universe, but it also gives a possible process for the formation of gravitational wave perturbations and cosmic density. We have calculated the cosmic parameters to studied cosmic inflation in HMPG.

We converted the  $f(\mathcal{X})$  theory to a scalar–tensor representation and described the scalar-field and the effective potential  $V(\varphi)$  in the form of the  $f(\mathcal{X})$  function. The *perturbed effective potential* yields  $R = -T + 2V_0$ . This model represents a de Sitter phase with  $V_0 \sim \Lambda$ , when  $T \sim 0$ , which is consistent with observations. We come up with a mathematical approach for HMPG to discuss inflation. To gain some insight, we graphically analyzed the characteristics of  $\alpha_s - n_s$  and  $r - n_s$  in Fig. 1, which are well-fitted with Planck-2018 data. Both of these characteristics have a significant role in determining the outcome of primordial density fluctuations.

We have also checked the effectiveness of  $f(\mathcal{X})$  gravity in describing the accelerating universe using the recent technique of irreversible matter creation process. We proposed a coherent and well ordered method that may describe the evolution of considered matter aspects (scalar-field and radiation field) in WIM by combining the fundamental principles of ITOS with the Einstein FEs in HMPG. The fundamental equations representing WIM can be numerically solved by using an adequate set of initial conditions for the related cosmological parameters. The solutions were calculated using HP,  $V(\varphi) = \pm \frac{v^2}{2}\varphi^2 + \frac{\xi}{4}\varphi^4$ . The corresponding solutions

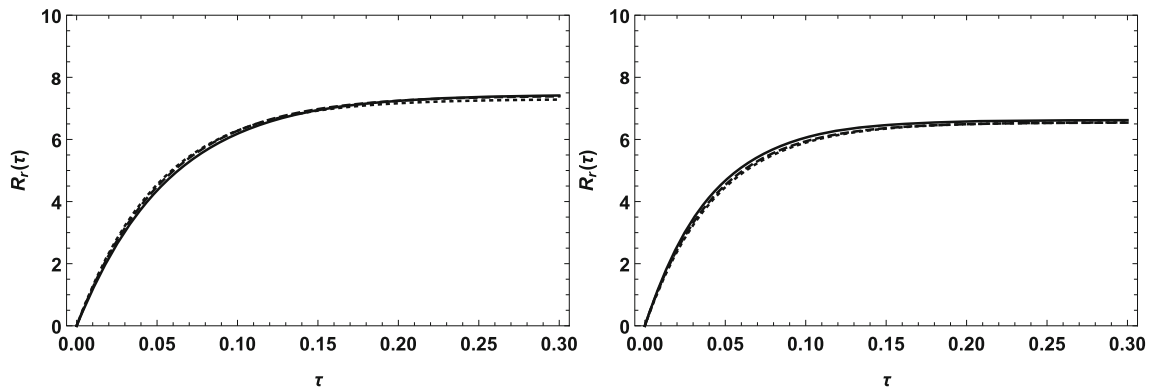


**Fig. 4** Above plots show the dimensionless radiation field  $R_\gamma$  versus dimensionless time. Left plot is for  $V(\varphi) = -\frac{v^2}{2}\varphi^2 + \frac{\xi}{4}\varphi^4$  and right plot is for  $V(\varphi) = +\frac{v^2}{2}\varphi^2 + \frac{\xi}{4}\varphi^4$ . Here we fixed the  $\sigma = 0.76$ ,  $\Gamma = 0.2$  with the different values of  $\epsilon$ ,  $\epsilon = 0.8$  (solid curve),  $\epsilon = 0.6$  (dashed curve) and  $\epsilon = 0.4$  (dotted curve)

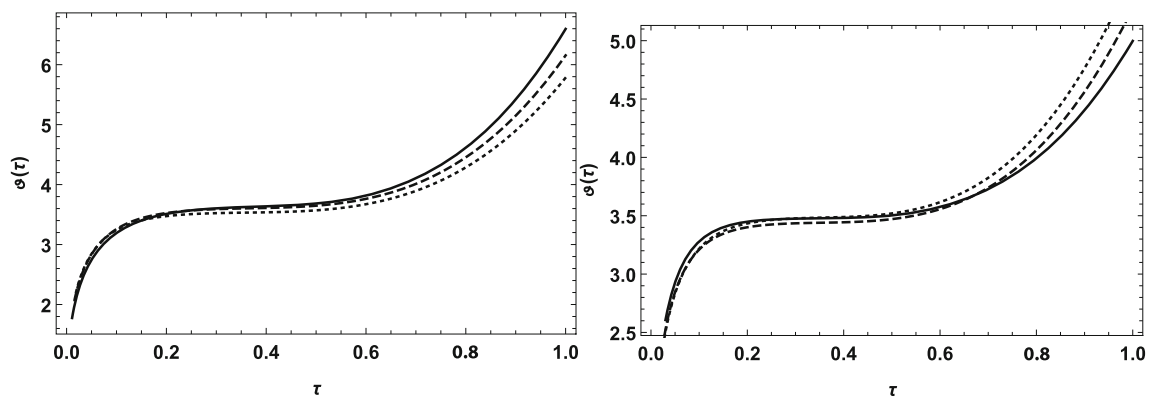


**Fig. 5** Above plots show dimensionless temperature  $\vartheta$  versus time. Left plot is for  $V(\varphi) = -\frac{v^2}{2}\varphi^2 + \frac{\xi}{4}\varphi^4$  and right plot is for  $V(\varphi) = +\frac{v^2}{2}\varphi^2 + \frac{\xi}{4}\varphi^4$ . Here we fixed the  $\sigma = 0.76$ ,  $\Gamma = 0.2$  with the different values of  $\epsilon$ ,  $\epsilon = 0.8$  (solid curve),  $\epsilon = 0.6$  (dashed curve) and  $\epsilon = 0.4$  (dotted curve)

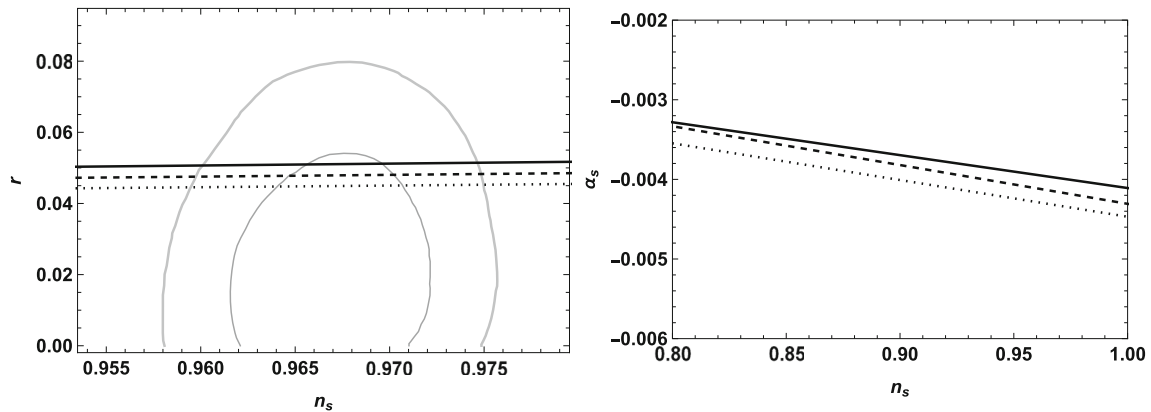


**Fig. 6** Left plot shows  $r$  versus  $n_s$  and right plot shows  $\alpha_s$  versus  $n_s$ . Here we fixed the  $\sigma = 0.76$ ,  $\Gamma = 0.2$  with the different values of  $\epsilon$ ,  $\epsilon = 0.8$  (solid),  $\epsilon = 0.6$  (dashed) and  $\epsilon = 0.4$  (dotted)

of differential equations are evaluated. The graphical representation of scale factor for both cases of HP is given in Fig. 2, which shows that  $a(t)$  is increasing exponentially with time. The graph of scalar-field particle number for both cases of HP is given in Fig. 3, both plots are showing decaying behaviour of  $N_\phi$  through cosmic evolution by changing the values of dimensionless parameter  $\varepsilon$ . In Fig. 4, the graph of dimensionless radiation field  $R_\gamma$ , which begins to increase and approaching to its maximum value with dimensionless time for both case of HP. In Fig. 5, the graph of dimensionless temperature  $\vartheta$  is slowly increasing over dimensionless time, after some short interval of time, the temperature is begin to increase rapidly. Finally, we have calculated the cosmic parameters for HP, which is necessary to describe the consistency with recent observational data in  $f(\mathcal{X})$  gravity. The  $r - n_s$  and  $\alpha - n_s$  graphs are showing in Fig. 6, which is well-fitted with Planck-2018 results.

It is worth mentioning here that the present paper is an extension of our previous work [39], which was an initial attempt to discuss inflation in  $f(\mathcal{X})$  gravity. Here, we extend it to discuss warm inflation, which is most effective phenomenon than simple inflation due to the involvement of temperature. To complete this analysis, we also discussed it from a thermodynamic point of view.

**Data Availability Statement** All data generated or analyzed during this study are included in this published article.

**Open Access** This article is licensed under a Creative Commons Attribution 4.0 International License, which permits use, sharing, adaptation, distribution and reproduction in any medium or format, as long as you give appropriate credit to the original author(s) and the source, provide a link to the Creative Commons licence, and indicate if changes were made. The images or other third party material in this article are included in the article's Creative Commons licence, unless indicated otherwise in a credit line to the material. If material is not included in the article's Creative Commons licence and your intended use is not permitted by statutory regulation or exceeds the permitted use, you will need to obtain permission directly from the copyright holder. To view a copy of this licence, visit <http://creativecommons.org/licenses/by/4.0/>.

Funded by SCOAP<sup>3</sup>. SCOAP<sup>3</sup> supports the goals of the International Year of Basic Sciences for Sustainable Development.

## References

- P.G. Bergmann, Int. J. Theor. Phys. **1**, 25–36 (1968)
- B.N. Breizman, V.T. Gurovich, V.P. Sokolov, Zh. Eksp. Teor. Fiz. **59**, 288 (1970)
- H.A. Buchdahl, Mon. Not. R. Astron. Soc. **150**, 1–8 (1970)
- A. Palatini, Rend. Circ. Mat. Palermo **43**, 203 (1919)
- G.J. Olmo, Int. J. Mod. Phys. D **20**, 413–462 (2011)
- T. Harko, T.S. Koivisto, F.S.N. Lobo, G.J. Olmo, Phys. Rev. D **85**, 084016 (2012)
- W. Hu, I. Sawicki, Phys. Rev. D **76**, 064004 (2007)
- S.A. Appleby, R.A. Battye, Phys. Lett. B **654**, 7 (2007)
- A.A. Starobinsky, JETP Lett. **86**, 157 (2007)
- S. Nojiri, S.D. Odintsov, Phys. Rep. **505**, 59 (2011)
- K. Bamba, S. Capozziello, S. Nojiri, S.D. Odintsov, Astrophys. Space Sci. **342**, 155 (2012)
- L. Amendola, R. Gannouji, D. Polarski, S. Tsujikawa, Phys. Rev. D **75**, 083504 (2007)
- P. Brax, Acta Phys. Polon. B **43**, 2307 (2012)
- T.S. Koivisto, D.F. Mota, M. Zumalacarregui, Phys. Rev. Lett. **109**, 241102 (2012)
- P. Brax et al., Rev. D **82**, 083503 (2010)
- P. Brax et al., Phys. Rev. D **86**, 044015 (2012)
- T. Koivisto, Phys. Rev. D **73**, 083517 (2006)
- G.J. Olmo, Phys. Rev. D **77**, 084021 (2008)
- A.A. Starobinsky, Phys. Lett. B **91**, 99 (1980)
- R. Myrzakulov, L. Sebastiani, S. Zerbini, Int. J. Mod. Phys. D **22**, 1330017 (2013)
- M. Zubair, F. Kousar, Can. J. Phys. **95**, 1074 (2017)
- F.C. Adams, J.R. Bond, K. Freese, J.A. Frieman, A.V. Olinto, Phys. Rev. D **47**, 426 (1993)
- K. Freese, W.H. Kinney, JCAP **1503**, 044 (2015)
- C.A. Picon, T. Damour, V.F. Mukhanov, Phys. Lett. B **458**, 209 (1999)
- G.R. Dvali, S.H.H. Tye, Phys. Lett. B **450**, 72 (1999)
- W. Zimdahl, J. Triginer, D. Pavon, Phys. Rev. D **54**, 6101 (1996)
- I. Prigogine, J. Gehehiau, E. Gunzig, P. Nardone, Proc. Natl. Acad. Sci. **85**, 7428 (1988)
- M. Calvão, J. Lima, I. Waga, Phys. Lett. A **162**, 223 (1992)
- J.A.S. Lima, A.S.M. Germano, Phys. Lett. A **170**, 373 (1992)
- T. Harko, F.S. Lobo, Int. J. Mod. Phys. D **13**, 2030008 (2020)
- C.G. Böhmner, F.S. Lobo, N. Tamanini, Phys. Rev. D **10**, 104019 (2013)
- S. Capozziello, T. Harko, T.S. Koivisto, F.S.N. Lobo, G.J. Olmo, Phys. Rev. D **12**, 127504 (2012)
- T. Harko, F.S. Lobo, H.M. da Silva, Phys. Rev. D **12**, 124050 (2020)
- N. Tamanini, C.G. Boehmer, Phys. Rev. D **8**, 084031 (2013)
- J.L. Rosa, S. Carloni, J.P. Lemos, F.S. Lobo, Phys. Rev. D **12**, 124035 (2017)
- R. Saleem, I. Shahid, Phys. Dark Univ. **35**, 100920 (2022)
- T. Harko, H. Sheikhahmadi, Phys. Dark Univ. **28**, 100521 (2020)
- S. Capozziello, T. Harko, T.S. Koivisto, F.S.N. Lobo, G.J. Olmo, JCAP **1304**, 011 (2013)
- H.R. Kausar, R. Saleem, A. Ilyas, Phys. Dark Univ. **26**, 100401 (2019)
- M. Fairbairn, M.H.G. Tytgat, Phys. Lett. B **546**, 1 (2002)
- L.M.H. Hall, I.G. Moss, A. Berera, Phys. Rev. D **69**, 083525 (2004)
- D. Samart et al., Eur. Phys. J. C **82**, 1–9 (2022)
- S. Capozziello, T. Harko, T.S. Koivisto, F.S.N. Lobo, G.J. Olmo, Universe **1**, 199 (2015)
- J. Hwang, H. Noh, Phys. Rev. D **54**, 1460 (1996)
- J. Hwang, Class. Quantum Gravity **14**, 1981 (1997)
- J. Hwang, Class. Quantum Gravity **15**, 1401 (1998)
- I.G. Moss, C. Xiong, JCAP **11**, 023 (2008)
- H. Mishra, S. Mohanty, A. Nautiyal, Phys. Lett. B **710**, 245–250 (2012)
- A. Kosowsky, M.S. Turner, Phys. Rev. D **52**, 1739 (1995)
- Y. Akrami et al., [Planck Collaboration], Planck 2018 results. X. (2018). [arXiv:1807.06211](https://arxiv.org/abs/1807.06211)
- N. Aghanim et al. [Planck Collaboration], Planck 2018 results. VI. [arXiv:1807.06209](https://arxiv.org/abs/1807.06209)
- G. Aad et al., ATLAS and CMS Collaborations, Phys. Rev. Lett. **114**, 191803 (2015)